Sex determination using 3D coordinate landmark data of the skull: a test using a CT sample

Robert D. Hoppa[1], Alexandra R. Klales[1], Laura J. Lidstone[1], Amy B. Scott[1], and Niels Lynnerup[2]
[1] Department of Anthropology, University of Manitoba ● [2] Department of Forensic Medicine, University of Copenhagen

Introduction

Increasingly, computed tomography (CT) imaging has become an accepted and more utilized non-invasive method in skeletal biology. For sex estimation and classification, CT data have been used to generate 3D skeletal models (3DCT) from which morphological features of the skull have been assessed. Furthermore, 3DCT is one method that may be used in conjunction with discrete 3D coordinate data points, which are commonly employed for craniometric assessment of sex.

Several studies have assessed the precision of 3DCT acquisition of landmarks as compared to traditional caliper measurements and coordinate data collected by use of a digitizer on actual skulls, and no significant differences were found (Hildebolt *et al.* 1990; Williams & Richtsmeier 2003). Additionally, no significant differences were found in tests of observer error for landmark designation (Richtsmeier *et al.* 1995), suggesting that coordinate data from CT scans can be reliably used for sex estimation.

The purpose of this study was to assess the validity of craniometric landmark generation from 3DCT scans for sex determination. Three areas were examined – the skull, the mandible and the orbits. Size and shape differences between the sexes were explored with 3D geomorphometric analysis.

Materials and Methods

The present analysis was conducted on a sample of post-mortem CT scans with documented sex, collected by the Department of Forensic Medicine, University of Copenhagen, although. The total sample size was 108 individuals (M=54, F=54) although this varied by individual analysis. Individuals were scanned at a voltage peak of 120 kVp with slice thickness varying between 0.5mm and 2.0mm.

Segmentation and rendering of the data was done using Materialise MIMICS medical imaging software to create 3DCT models of the skull for each individual. From the 3DCT, landmarks of the skull (n=21), mandible (n=19) and orbits (n=16) were placed on the 3D rendered skulls. The coordinate data for each landmark and for each individual were then exported from MIMICS to PAST (PAleontological STatistics) software (Hammer *et al.* 2001) and SPSS statistical software programs for further analyses.

The landmark data for each analysis were subjected to a Procrustes transformation and were then analyzed using discriminant function analysis with a leave-one-out approach to assess determination of sex.

Table 1. Alphabetized list of abbreviations for landmarks (after Moore-Jansen et al. 1994).
**Left and right sides collected.*

Abbrev	Landmark Name
AL	Alare*
AU	Auriculare*
B	Bregma
BA	Basion
D	Dacryon*
EC	Ectoconchion*
EU	Euryon*
FMB	Foramen Magnum*
	Frontomalare
FMT	Temporale*
FT	Frontotemporale*
G	Glabella
GN	Gnathion
GO	Gonion*
ID	Infradentale
L	Lambda
N	Nasion
NS	Nasospinale
O	Opisthion
OP	Opisthocranion
PR	Prosthion
ZY	Zygion*

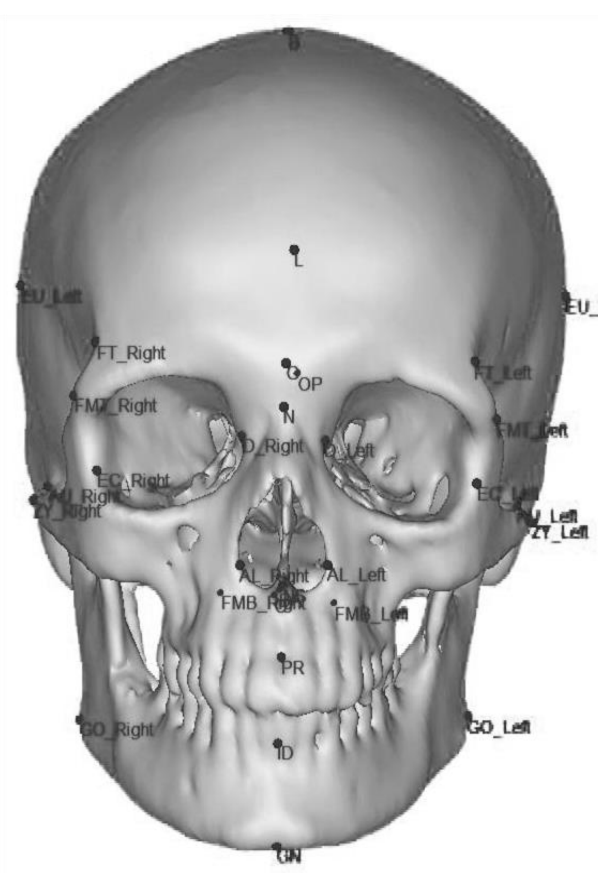

Figure 1. 3DCT skull model with landmarks designated.

Methods cont.

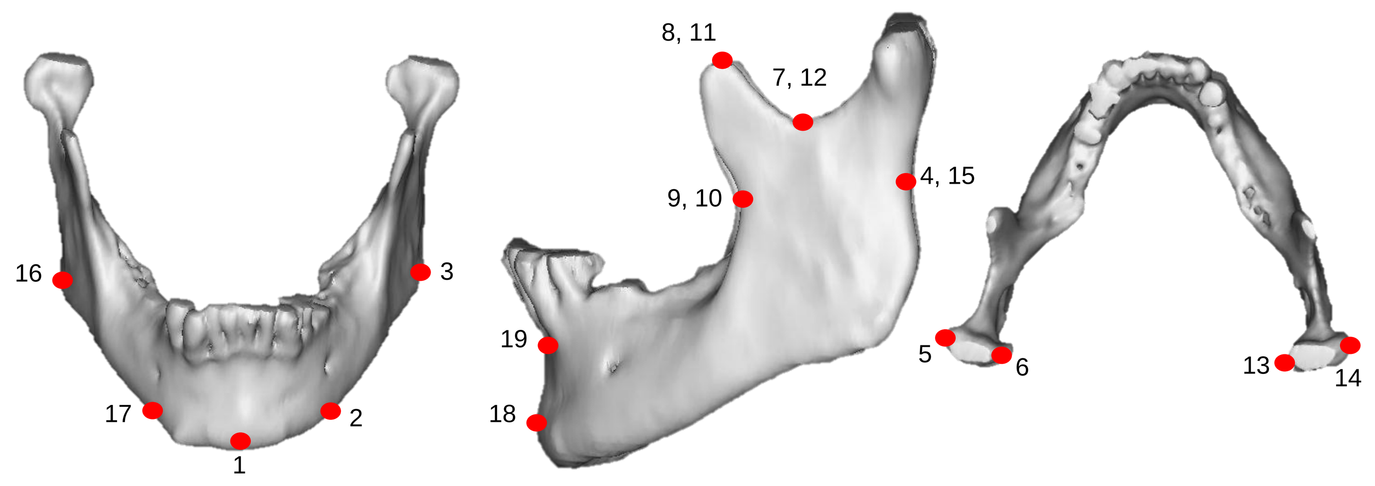

Figure 2. 3DCT models of the mandible with landmarks shown.

Table 2. List landmarks collected (after Franklin, O'Higgins and Oxnard 2008; Buikstra and Ubelaker 1994).

Landmark	Description
1. Gnathion	most inferior point of the mandible in the sagittal plane
2. Mental foramen line (left)	line draw perpendicular from the mental foramen to the inferior border of the mandible
3. Gonion (left)	most lateral inferior point on mandible at the junction of the ascending ramus
4. Posterior ramus (left)	point at which there is the most concavity along the posterior ramus
5. Condylion laterale (left)	most lateral point on the condyle
6. Condylion mediale (left)	most medial point on the condyle
7. Mandibular notch (left)	most inferior point between the condyle and coronoid process
8. Coronion (left)	most superior point on the coronoid process
9. Anterior ramus (left)	point at which there is the most concavity along the anterior ramus
10. Anterior ramus (right)	point at which there is the most concavity along the anterior ramus
11. Coronion (right)	most superior point on the coronoid process
12. Mandibualr notch (right)	most inferior point between the condyle and coronoid process
13. Condylion mediale (right)	most medial point on the condyle
14. Condylion laterale (right)	most lateral point on the condyle
15. Posterior ramus (right)	point at which there is the most concavity along the posterior ramus
16. Gonion (right)	most lateral inferior point on mandible at the junction of the ascending ramus
17. Mental foramen line (right)	line draw perpendicular from the mental foramen to the inferior border of the mandible
18. Pogonian	most projecting point of the chin along the sagittal plane
19. Mandibular symphysis	most concave point of the mandibular symphasis along the sagittal plane

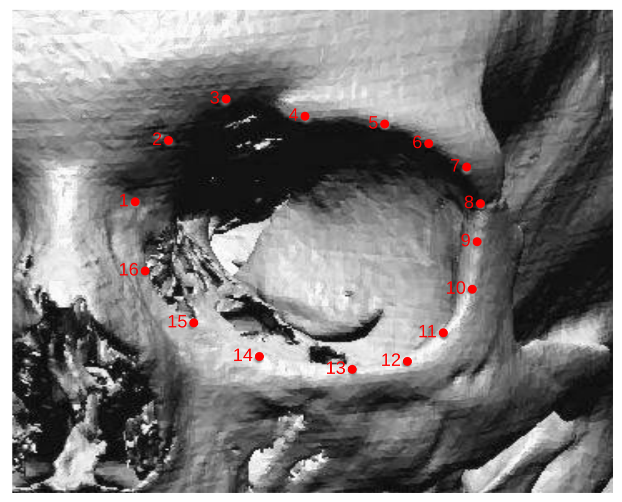

Figure 3. 3DCT model of the orbital area with landmarks shown.

Table 3. List landmarks and pseudolandmarks collected on the orbits

Landmark	Description
1.	Dacryon
2.-4.	Along orbital margin between dacryon and superior orbital border point
5.	Superior orbital border
6.-8.	Along orbital margin between superior orbital border and ectoconchion
9.	Ectoconchion
10.-12.	Along orbital margin between ectoconchion and orbitale
13.	Orbitale
14.-16.	Along orbital margin between orbitale and dacryon

Results

The results of the discriminant function analysis for each of the three areas is presented graphically and in tabular format. The cross-validated accuracies are a more realistic reflection of the ability to reliable predict sex from the suite of landmarks.

Table 4. Accuracy and cross-validated accuracy for determination of sex from the orbital landmarks using stepwise discriminant functions analysis.

Classification Results for orbital landmarks[b,c]

		Sex	Predicted Group Membership: Female	Predicted Group Membership: Male	Total
Original	Count	Female	45	6	51
		Male	12	36	48
	%	Female	88.2	11.8	100.0
		Male	25.0	75.0	100.0
Cross-validated[a]	Count	Female	45	6	51
		Male	12	36	48
	%	Female	88.2	11.8	100.0
		Male	25.0	75.0	100.0

a. Cross validation is done only for those cases in the analysis. In cross validation, each case is classified by the functions derived from all cases other than that case.
b. 81.8% of original grouped cases correctly classified.
c. 81.8% of cross-validated grouped cases correctly classified.

Table 5. Accuracy and cross-validated accuracy for determination of sex from the mandibular landmarks using stepwise discriminant functions analysis.

Classification Results for mandibular landmarks[b,c]

		Sex	Predicted Group Membership: Female	Predicted Group Membership: Male	Total
Original	Count	Female	36	6	42
		Male	8	36	44
		Ungrouped cases	1	0	1
	%	Female	85.7	14.3	100.0
		Male	18.2	81.8	100.0
		Ungrouped cases	100.0	.0	100.0
Cross-validated[a]	Count	Female	34	8	42
		Male	10	34	44
	%	Female	81.0	19.0	100.0
		Male	22.7	77.3	100.0

a. Cross validation is done only for those cases in the analysis. In cross validation, each case is classified by the functions derived from all cases other than that case.
b. 83.7% of original grouped cases correctly classified.
c. 79.1% of cross-validated grouped cases correctly classified.

Results cont.

Table 5. Accuracy and cross-validated accuracy for determination of sex from the mandibular landmarks using stepwise discriminant functions analysis.

Classification Results for cranial landmarks[b,c]

		Sex	Predicted Group Membership: Female	Predicted Group Membership: Male	Total
Original	Count	Female	46	8	54
		Male	7	43	50
	%	Female	85.2	14.8	100.0
		Male	14.0	86.0	100.0
Cross-validated[a]	Count	Female	44	10	54
		Male	9	41	50
	%	Female	81.5	18.5	100.0
		Male	18.0	82.0	100.0

a. Cross validation is done only for those cases in the analysis. In cross validation, each case is classified by the functions derived from all cases other than that case.
b. 85.6% of original grouped cases correctly classified.
c. 81.7% of cross-validated grouped cases correctly classified.

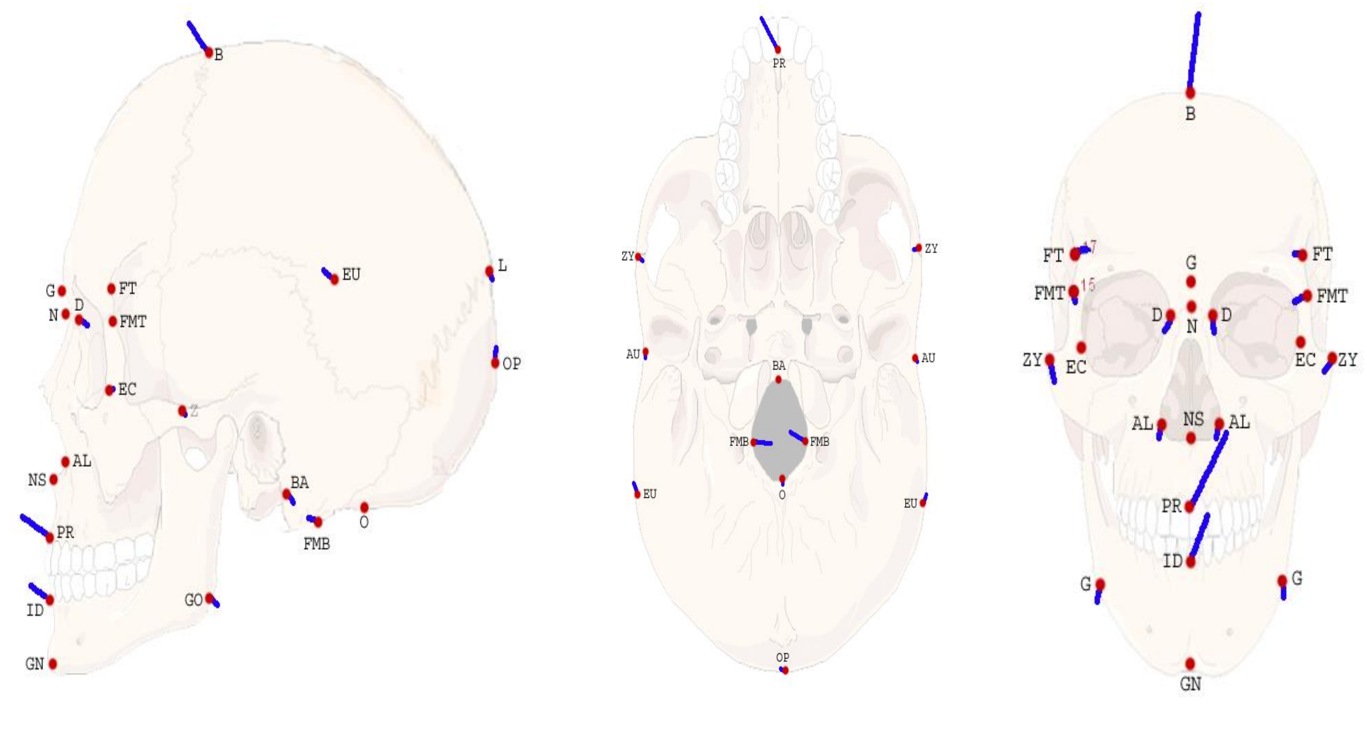

A B C

Figure 4. Mean landmark points for males and females in A) lateral view, B) inferior view, C) anterior view (photo from Wilkens & Williams 2001).

Discussion and Conclusions

In general, all areas show discrimination of sex in excess of 80% accuracy. However, when cross-validated using leave-one-out analysis, accuracy is more conservative between 79.1% and 81.8%. For both the orbital and mandibular landmarks, females classified slightly better than males. Based on the greater displacement of the landmarks shown in Figure 4, males were generally more prognathic in the mouth region and tended to have larger shape differences in the width of the foramen magnum and in cranial breadth than females (Klales et al. 2011).

While good levels of accuracy were observed using 3D landmarks on the cranium, such data need to be collected in digital format (using a digitizer or 3D renders from CT data) and subsequently processed before being of practical use. This perhaps makes it less convenient when a quick assessment of a single individual in the lab or field is desirable, but remains of value for broader studies of sexual dimorphism in populations or when a highly detailed osteobiography of remains is warranted.

References

Buikstra, J. and D. Ubelaker, 1994. Standards for Data Collection from Human Skeletal Remains. Fayetteville: Arkansas Archaeological Survey.
Franklin, D., P. O'Higgins and C. Oxnard, 2008. Sexual dimorphism in the mandible of indigenous South Africans: A geometric morphometric approach. South African Journal of Science, 104, pp. 101-106.
Hammer Ø, Harper DA, Ryan PD. 2001. PAST: Paleontological Statistics Software Package for Education and Data Analysis. *Palaeontologia Electronica* 4:1-9.
Hildebolt CF, Vannier MW, Knapp, RH. 1990. Validation Study of Skull Three-Dimensional Computerized Tomography Measurements. *American Journal of Physical Anthropology* 82:283-294.
Klales AR, Lynnerup N and Hoppa RD (2011) Geometric Morphometric Analysis of Sex Determination from Cranial Landmark Data Using Computed Tomography. Poster presented at the 39th Annual Meetings of the Canadian Association for Physical Anthropology, Montreal, Oct 2011.
Moore-Jansen PH, SD Ousley, and RL Jantz. 1994. Data Collection Procedures for Forensic Skeletal Material (3rd ed.). Knoxville, Tennessee: University of Tennessee Forensic Anthropology Series.
Richtsmeier JT, Paik CH, Elfert PC, Cole III TM, Dahlman HR. 1995. Precision, Repeatability, and Validation of the Localization of Cranial Landmarks using Computed Tomography Scans. *Cleft-Palate Craniofacial Journal* 32:217-227.
Wilkens L, Williams B. 2001. Smart Draw LifeART collection images. Retrieved 17 October 2011 from <www.smartdraw.com>.
Williams FL, Richtsmeier JT. 2003. Comparison of Mandibular Landmarks from Computed Tomography and 3D Digitizer Data. *Clinical Anatomy* 16:494-500.

Acknowledgements

This research was supported in part by the Canada Research Chairs program. Other funding support includes University of Manitoba Graduate Fellowships, Manitoba Graduate Scholarships and the Dr. Emőke Szathmáry Graduate Fellowship in Biological Anthropology.

Social Sciences and Humanities Research Council of Canada | Conseil de recherches en sciences humaines du Canada | Canada